INFLUENCE OF SPECIMEN GEOMETRY ON THE FATIGUE BEHAVIOR OF A CARBON FABRIC REINFORCED PPS

I. De Baere[1*], W. Van Paepegem[1], J. Degrieck[1]

[1]Mechanics of Materials and Structures, Department of Materials Science and Engineering University, Technologypark-Zwijnaarde 903, B-9052 Zwijnaarde, Belgium
*Ives.DeBaere@UGent.be

Keywords: Fatigue, Dumbbell, Dog bone, FEM.

Abstract
This manuscript studies the tension-tension fatigue behavior of a carbon fabric reinforced PPS and the influence of the specimen geometry on the obtained results. First, the fatigue experiments are preformed according to the ASTM D3479/D3479M standard using the rectangular shaped specimen, but virtually all specimens fail in the tabbed section. This, however, means that fatigue lifetime may be underestimated. Therefore, a new dumbbell-like shape was assessed. Based on the occurring stress concentrations in the tabbed section, the dog bone-like shape was first optimised numerically using FEM, and then, the optimised specimen was tested in tension-tension fatigue. It can be concluded that this dumbbell shape yields better results in terms of acceptable failure and that the used shape has a significant influence on the fatigue lifetime.

1. Introduction

Investigating the fatigue behavior of a material is often a very long-lasting and cumbersome procedure. Not only do some of the experiments last very long, in most cases the scatter on the results is fairly large, meaning that most experiments need to be repeated a number of times in order to achieve statistically significant results. However, one event may happen quite regularly, can be unexpected but compromises the fatigue lifetime data, namely tab failure. The ASTM D3479/D3479M – 96(2007) '*Standard Test Method for Tension-Tension Fatigue of Polymer Matrix Composite Materials*' mentions that 'premature failure of the specimen in the tab region is common in tension-tension fatigue testing…' and that 'a combination of tab material, tab length and adhesive that minimizes tab failures' should be found using a set of preliminary fatigue tests. If tab failure happens occasionally, then it is not really a problem, but if this optimal end tab configuration cannot be found, or does not exist, then it is very hard to obtain valid fatigue lifetime results.

In this manuscript, the tension-tension fatigue behavior of a carbon fabric reinforced thermoplastic, namely polyphenylene sulphide, will be assessed (i) using the rectangular specimen geometry, as imposed by the ASTM D3479/D3479M Standard and (ii) using an optimized dumbbell like shape. Due to the nature of this material, tab failure is likely to occur [1] using the rectangular shape. It was first attempted to find the optimal end tab configuration, but nevertheless, not too much attention will be given to the number of cycles till failure in the case of tab failure, since this will always be an underestimation.

1

Besides the influence of the specimen geometry, the macro-mechanical behavior of the material under fatigue loadings will also be assessed. With respect to damage occurring throughout the fatigue lifetime, many forms are possible in fiber-reinforced composites [2]. This damage affects the value of the elastic properties at an early stage. Especially in fatigue, the damage initiation phase can cause a decrease of the elastic modulus of 5 to 10 %. In the next damage propagation phase, the stiffness continues to decrease gradually, ranging from a few percent for unidirectionally reinforced carbon composites to several tens of percents for multidirectional glass laminates [3, 4]. Furthermore, most one-dimensional damage models for fiber reinforced composites only account for the effect of damage on the stiffness [2, 5, 6]. As such, the main focus in the fatigue experiments described here is on the stiffness degradation and permanent deformation.

2. Materials and methods

The composite material used for the experiments was a 5-harness satin weave carbon fabric reinforced polyphenylene sulphide (PPS). The carbon PPS plates were hot pressed at 300°C and 10 bar and one stacking sequence was used for this study, namely $[(0°,90°)]_{4s}$. The in-plane elastic properties and the tensile strength properties are listed in Table 1. This material was supplied to us by Ten Cate Advanced Composites (The Netherlands).

E_{11} [GPa]	E_{22} [GPa]	ν_{12} [-]	G_{12} [GPa]	X_T [MPa]	ε_{11}^{ult} [-]	Y_T [MPa]	ε_{22}^{ult} [-]	S_T [MPa]
56.0	57.0	0.033	4.175	736	0.011	754.0	0.013	110.0

Table 1 Elastic and strength properties of the CETEX® material

All tensile tests were performed on a servo-hydraulic INSTRON 8801 tensile testing machine with a FastTrack 8800 digital controller and a load cell of ±100kN. All quasi-static experiments were done displacement-controlled at a speed of 2 mm/min, whereas all fatigue tests were done in load-controlled mode with a minimum stress of 0 MPa and a certain maximum σ_{max} at a given frequency. For the registration of the tensile data, a combination of a National Instruments USB 6251 data acquisition card and the SCB-68 pin shielded connecter were used. The load, displacement and strain, given by the FastTrack controller were sampled on the same time basis.

3. Rectangular specimen

3.1. Quasi-static testing

As mentioned in the introduction, an extensive amount of tests were conducted to determine the optimal combination of end-tab geometry (straight or chamfered), end-tab material (GFRP, CFRP, Aluminum), end-tab stacking sequence, surface preparation and type of adhesive [9] to be used with the rectangular specimen of   250 mm x 30 mm x 2.5 mm. However, none resulted in an acceptable failure, meaning that failure occurred in (or near) the centre of the specimen. Also, some results proved highly irreproducible, when multiple experiments were performed. Therefore, an extensive numerical study was conducted to obtain the best end tab combination for this material and to determine the reason for the end tab failure [1]. From this study, it was concluded that for the given material, straight end tabs with the same stacking sequence yields the best results, but in every case (straight or chamfered tabs, different tab materials, …) stress concentrations exist underneath the tabs, so with the geometry from the D3479/D3479M – 96 (2007) '*Standard Test Method for Tension-Tension Fatigue of Polymer Matrix Composite Materials*' and D3039/D3039M-00 '*Standard Test Method for Tensile Properties of Polymer Matrix Composite Materials*' tab failure is

very likely to occur for the $[(0°,90°)]_{4s}$ stacking sequence of the carbon PPS under study. Figure 1 illustrates the occurring longitudinal stress concentration when straight end tabs are used for various end tab materials, the value R_A represents the gripping force; for more details, the authors refer to [1].
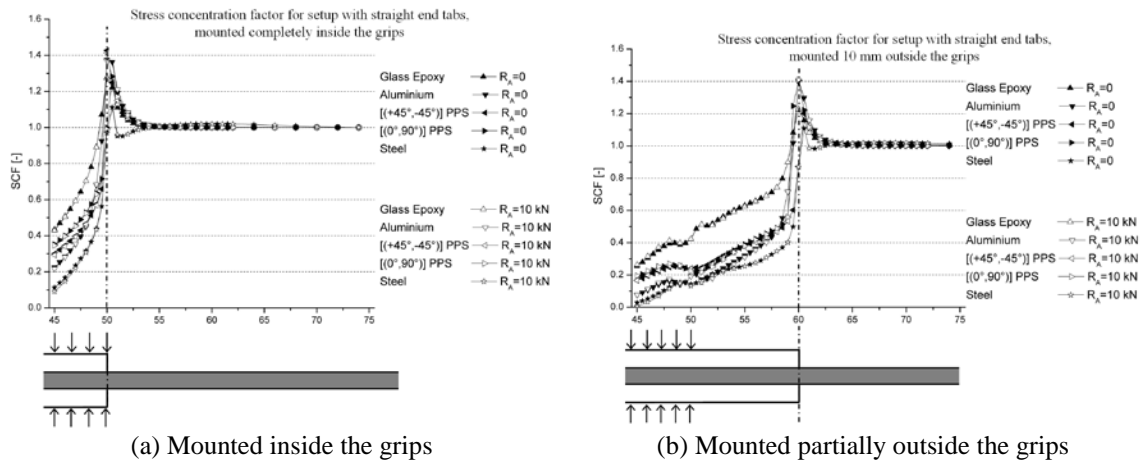

(a) Mounted inside the grips   (b) Mounted partially outside the grips

Figure 1 Illustration of the stress concentration factor for the longitudinal stress for straight end tabs [1].

3.2.   Fatigue loading

Figure 2 shows the results of a fatigue experiment between 0 and 550 MPa at a 5Hz loading frequency. The latter was chosen as a compromise between the expected heat generation and the duration of the experiment. In order to evaluate the stiffness degradation, the experiment was paused regularly to perform quasi-static tests (Figure 2(b)). However, no real stiffness degradation occurred during the test and there was only very limited permanent deformation. It should also be noted that there was no significant change in temperature. The test specimen failed after 1,217,500 cycles and failure occurred in the end tabs, meaning fatigue life is underestimated.
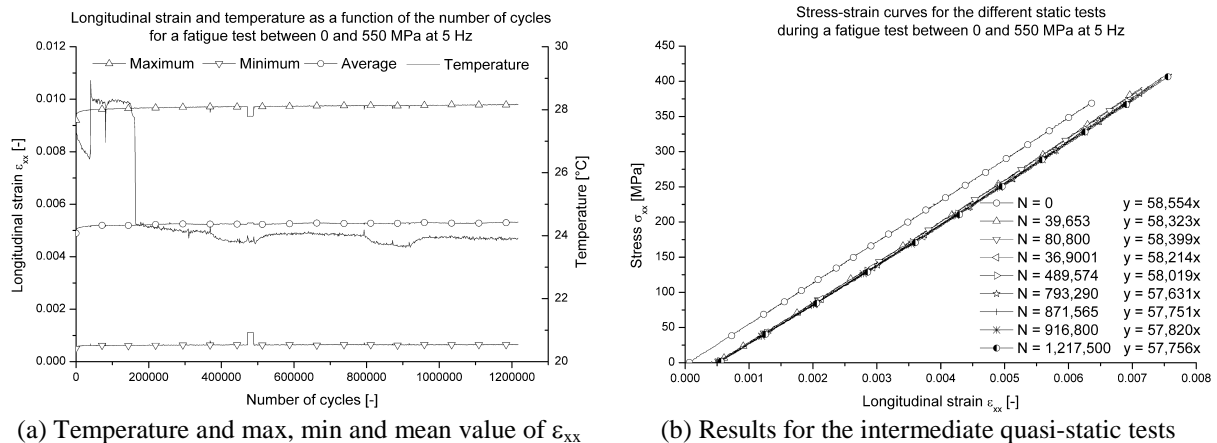

(a) Temperature and max, min and mean value of ε_{xx} (b) Results for the intermediate quasi-static tests

Figure 2 Illustration of the results on the rectangular specimens of a 550 MPa@5Hz fatigue experiment.

A remark must be made concerning the mentioned fatigue lifetime. The experiment showed here failed after about 1.2 million cycles and a few others also survived one million cycles or failed soon afterwards. However, multiple specimens failed very early in the expected fatigue life, due to tab failure, caused by the already mentioned stress concentrations, inherent to the used geometry [1]. Furthermore, the failure of the adhesive layer, causing debonding of the tab also results in failure. The latter causes friction and wear to occur and the generated heat causes the premature failure. Moreover, due to the debonding, the stress concentration shifts

to the edge of the debonded zone, since the stress concentration occurs at the edge of this zone (see Figure 1). As such, specimens which fail during or soon after the run in, usually fail just outside the end tabs, whereas specimens which last longer, usually fail inside the end tabs, although this also depends on the quality of the bond. The occurring failures are illustrated in Figure 3.

(a) during run-in   (b) soon after run-in/good bond   (c) late in fatigue life/bad bond

Figure 3 Overview of the occurring tab failures during fatigue experiments

Almost all experiments with higher maximum stress levels of 575 MPa and 600 MPa failed during or soon after the run-in in the tabbed section, so these results are not shown here. For more fatigue results at different load levels and different loading frequency, the authors refer to [9].

4. Specimen geometry

4.1. Theoretical deduction

In a previous study [1], the stress concentration factors underneath the end tabs were determined and it was concluded that straight edged tabs with $[(0°,90°)]_{4s}$ stacking sequence, mounted completely inside the grips, gave best results for the material under study, when both experiments and finite element simulations are taken into account. This strategy yields a stress concentration factor as result of the tabs (s_t) of 1.3. The idea here is to have a slight curvature of the specimen, so that this stress concentration is compensated by having a less wide specimen. This is shown in Figure 4. It should be noted that the geometry differs from the ones mostly found in literature: in most cases, there is a constant section in between the two curved areas [7], whereas here, the curved section has a constant radius and thus a constantly varying width. The reason for the constant radius will become clear in the finite element assessment.
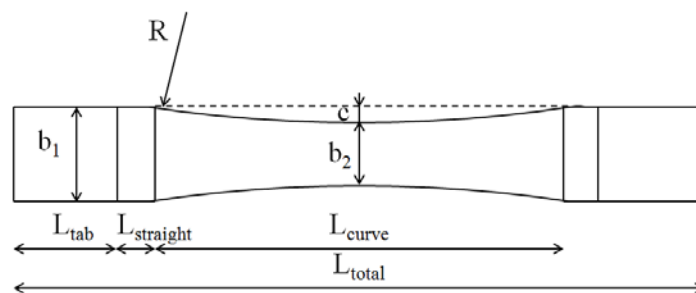

Figure 4 Illustration of the proposed dog bone shape.

By using simple mathematics [8], it is quite easy to derive the following formula for the radius R [mm], with s_t [-] the stress concentration factor resulting from the tabs:

$$R = \frac{\left(\frac{s_t-1}{s_t}\right)^2 b_1^2 + l_{curve}^2}{4\left(\frac{s_t-1}{s_t}\right) b_1} \qquad (1)$$

4

As a result, using a given L_{curve} and a given width b_1, Equation 1 yields a lower boundary for the necessary radius to obtain the stress in the middle of the specimen being equal or higher than the stress concentration underneath the tabs, with given stress concentration factor s_t. It is hereby assumed that there is no stress concentration due to the curvature of the dog bone, only the stress concentration underneath the end tabs is taken into account. However, it is expected that a small stress concentration as result of the radius might be present, meaning that the stresses in the centre of the specimen will be even higher than underneath the end-tabs. As such, there is an extra safety factor of failure occurring in the curved zone, rather than underneath the tabs.

In order to determine an interesting set of dimensions, there are two possible procedures: (i) experimentally test different geometries and verify which geometry gives the best results or (ii) model the geometry in finite element software and asses the geometry numerically. The authors have chosen the second option, which is described next.

4.1.1. Finite element results

Figure 5 shows the longitudinal stress σ_{xx} for several simulations. A specimen with $L_{curve} = 100$ with a corresponding radius of 362.8 mm is illustrated in Figure 5.1. As was expected, the stresses increase towards the centre of the specimen, but a fairly large stress concentration is present near the centre of the specimen. This is depicted in Figure 5.1 (b) in more detail with an adjusted scale.
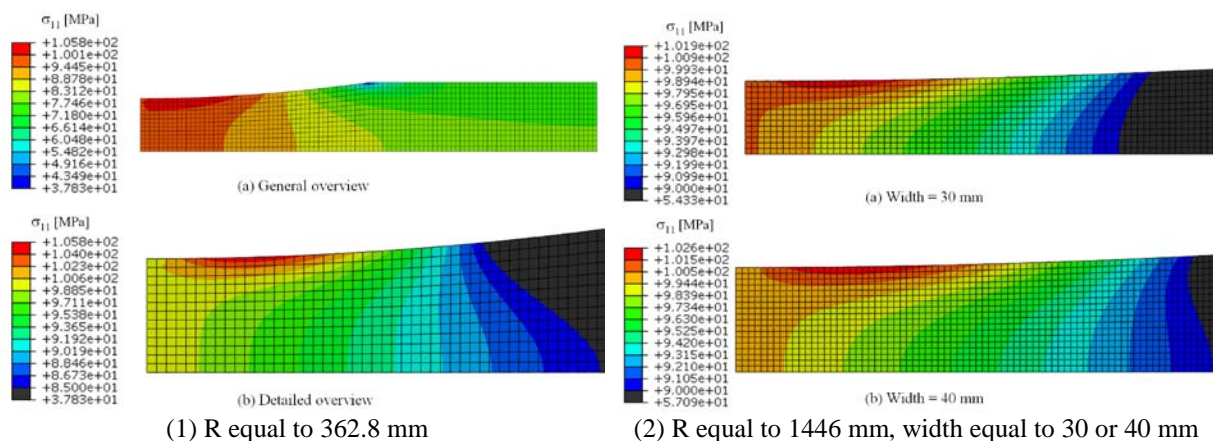

(1) R equal to 362.8 mm   (2) R equal to 1446 mm, width equal to 30 or 40 mm

Figure 5 Longitudinal stress for the dog bone

From the results in Figure 5.1, the stress concentration factor s_{curve} can be calculated and yields a value of 1.058. This also explains why in [7] for their 0° lay-up, the failure occurred just after the circular section in the smallest cross-section of their dumbbell specimen. It is expected that for longer curved sections, the stress distribution will be more smoothly. This was verified by simulating a geometry with a length of 400 mm. Indeed, the stress distribution is smoother than the previous simulation and the stress concentration is negligible. For this case, a stress concentration factor s_{curve} of 1.009 is found. However, a specimen of 400 mm is already quite long and will yield rather large displacements during fatigue tests with maximum strains around 1%. Therefore, a total length of 300 mm is considered next. In order to evaluate the effect of the width of the specimen, both 30 mm and 40 mm are considered. These results are illustrated in Figure 5.2, only the detailed overviews are given. It can be noted that increasing the width for a given curved length increases the value and size of the stress concentration. For these geometries, stress concentration factors of 1.019 and 1.026 are found for 30 mm and 40 mm width respectively.

5

Finally, one could state that because the width is not constant in the centre of the specimen, there will be a variation in the longitudinal strain in that area. Since the strain will be measured with an extensometer during the fatigue experiments, this could influence the measurement because this device measures the strain over a certain length and therefore averages out the variations. However, it was verified that a uniform strain field was present over the gauge length of the extensometer [8]. More details of the finite element model can also be found in [8].

5. Experiments and Discussion

Now that the dimensions of the specimen are fixed, the geometry can be validated experimentally. In the next paragraph, quasi-static tests are discussed and then, fatigue experiments are conducted.

5.1. Quasi-static testing

Previous experiments with rectangular specimens, done by the authors yielded average failure stresses between 600 and 700 MPa, with occasionally a value higher than 700 [9]. However, in almost all cases, failure occurred in the tabbed section. Figure 6 (a) shows the σ_{xx} as function of ε_{xx} for two experiments with R = 1446 mm. The second curve is given an offset along the x-axis for a better view. It should be noted that the derived stiffness corresponds well with the values determined with the resonalyser method (Table 1), meaning that the slightly non-uniform strain field does not corrupt the extensometer measurement. Around 700 MPa, the extensometer was removed to avoid damage of this device when the specimen fails. The experiments, however, were then continued to determine the failure stress.
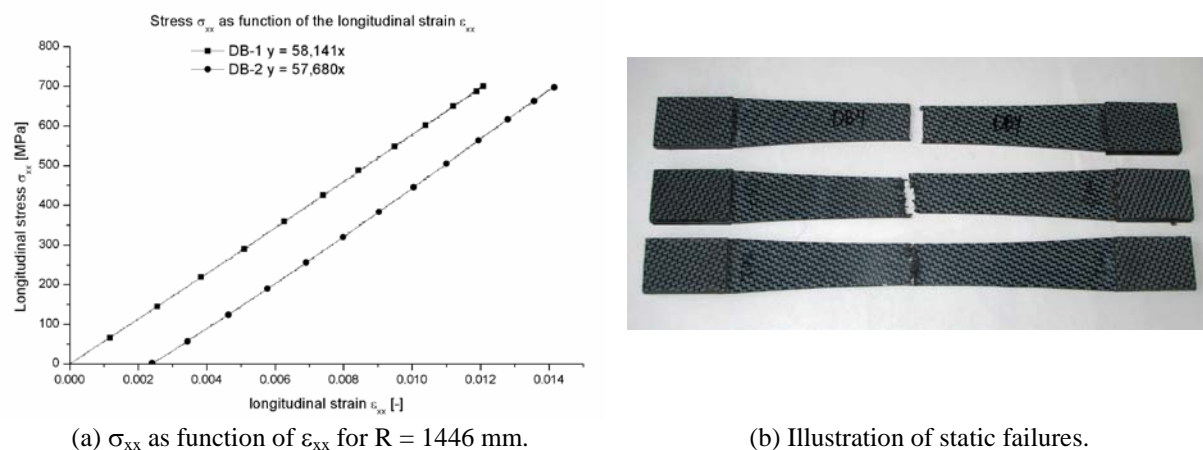

(a) σ_{xx} as function of ε_{xx} for R = 1446 mm.　　　　　(b) Illustration of static failures.

Figure 6 Overview of quasi-static experiments

Not all experiments are shown here, but for all five conducted quasi-static experiments, an average failure stress of 768.8 MPa was found, the maximum achieved stress was 828 MPa, but both values are significantly higher than the ones achieved with the rectangular shaped specimens. Figure 6 (b) illustrates some of the failed specimens. It should be noted that failure does not occur exactly in the centre of the specimen, but slightly above. This, however, is the location of the stress concentration for this geometry (see Figure 5) and was therefore predicted. It can be remarked that the entire geometry is in fact based on the stress concentration factor of 1.3, which was previously derived using finite element modeling. It is of course possible that this factor may overestimate the real stress concentration. Therefore, two extra geometries, corresponding to two lower stress concentration factors, namely 1.2 and 1.1, were also considered, yielding a radius of R = 2001 mm and R = 3667 mm respectively. Both geometries were tested, but both always failed in or underneath the end tabs; the

corresponding failure stresses, however, where in the same order of magnitude than for the R =1446 mm geometry.
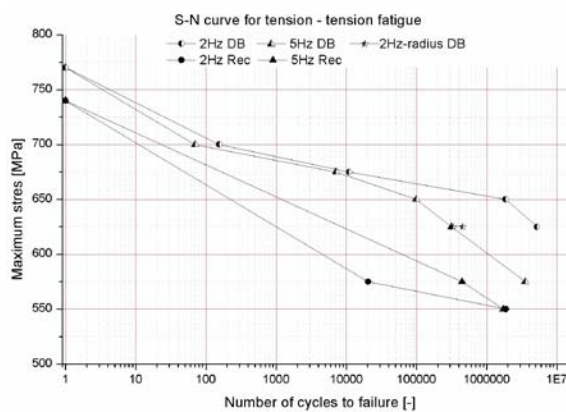
5.2. Fatigue experiments

Both 2 Hz and 5 Hz experiments were conducted and since the quasi-static experiments already yielded promising results, a first fatigue test was conducted with σ_{max} = 575 MPa at 5 Hz. This test survived over 3.6 million cycles and failed little above the centre of the specimen, which is a huge difference with the results from the previous fatigue study with rectangular specimens [9], where a maximum stress level of 575 MPa almost always resulted in tab failure during run-in of the experiment. Other experiments with σ_{max} equal to 625, 650, 675 and 700 MPa at both 2 Hz and 5 Hz were conducted. All of the specimens with R = 1446 mm failed just above the centre of the specimen, again as predicted in the finite element simulations.

During the fatigue life, all specimens showed a similar behavior. Figure 7 (a) shows the evolution of the maximum, minimum and average value of the longitudinal strain during a 625 MPa@2Hz fatigue test. As can be seen, there is only limited permanent deformation, of which most occurs earlier in fatigue life. The difference between minimum and maximum strain level does not change significantly and given the fact that it is a load controlled test, this means that almost no stiffness degradation occurs. Around 1.8 million cycles, the rubber bands, holding the extensometer to the specimen, ruptured, so no strain data after this event is present. However, when observing the displacement during this test, a similar trend till failure at around 6 million cycles is present. Again, no significant rise in temperature was noted.

Similar to the static tests, also the geometries corresponding to the stress concentration factor of 1.2 and 1.1 were also tested under fatigue loading conditions. On both types, a 625 MPa@2Hz fatigue test was conducted, but both specimens failed in the tabbed section and compared to the dog bone with the 1446 mm radius, fatigue life is underestimated. Nevertheless, one could make the remark that both these geometries yield significantly higher fatigue life than with the rectangular specimens, where 625 MPa could not even be reached under fatigue loading conditions.
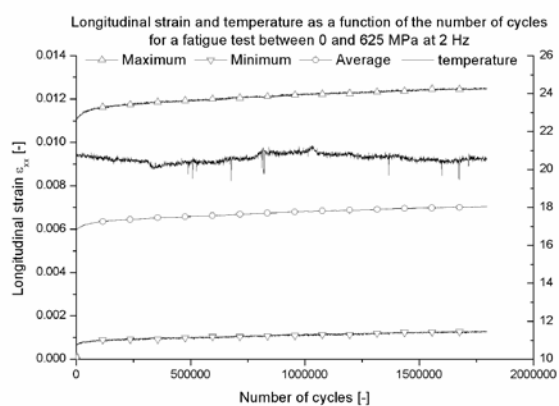
(a) Temperature and max, min and mean value of ε_{xx} during a 625 MPa@2Hz fatigue experiment.

(b) Maximum cycling stress as function of the fatigue life for 2 Hz and 5 Hz experiments.

Figure 7 Illustration of the fatigue results.

To summarize, Figure 7 (b) gives an overview of the maximum stress level and corresponding fatigue life for both geometries. The experiments for the different stress concentration factors are also depicted (2Hz-radius DB). Apparently, there is only little influence of the frequency on the fatigue life for higher stress levels, whereas for stress levels lower than 675 MPa, a lower frequency yields a larger number of cycles to failure. For comparison purposes, the experiments with the rectangular shape specimens with the longest fatigue life are also added,

but it is quite clear that the dog bone shape is superior. It should be noted that for the stress levels between 575 and 740 MPa, all rectangular specimens failed during run in, so no data as available.

6. Conclusions

In this manuscript, the tension-tension fatigue behavior of a carbon fabric reinforced PPS was assessed by using a rectangular and a dumbbell like shape. The latter was first optimized by FEM based on the occurring stress concentration underneath the end tab. Compared to the rectangular specimens, the quasi-static tests yielded higher failures stresses. Under fatigue loading conditions, it appears that with the rectangular shape, fatigue life is highly underestimated and with the dog bone, higher maximum load levels were possible. Furthermore, the specimen always failed just above the centre of the sample, as predicted by the simulations.

With respect to the fatigue behavior, very little permanent deformation manifests itself and it mainly occurs early in fatigue life; very little stiffness degradation is present and there is no significant increase in temperature. Furthermore, there is only little influence of the frequency on the fatigue life for higher stress levels, whereas for stress levels lower than 675 MPa, a lower frequency yields a larger number of cycles to failure.

Acknowledgements

References

[1]   De Baere I., Van Paepegem W. and Degrieck J. On the design of end tabs for quasi-static and fatigue testing of fibre-reinforced composites. *Polymer Composites,* **30** (4), pp 381-390 (2009).

[2]   Talreja, R. Damage and fatigue in composites - A personal account. *Composite Science and Technology,* **68** (13) pp 2585-2591 (2008).

[3]   Schulte, K., Baron, Ch., Neubert, H., Bader, M.G. , Boniface, L., Wevers, M., Verpoest, I. and de Charentenay, F.X. (1985). *Damage development in carbon fibre epoxy laminates : cyclic loading* in "Proceedings of the *MRS-symposium "Advanced Materials for Transport"*, Strassbourg, France. (1985)

[4]   Schulte, K., Reese, E. and Chou, T.-W. (1987). *Fatigue behavior and damage development in woven fabric and hybrid fabric composites* in proceedings of the "*Sixth International Conference on Composite Materials (ICCM-VI) & Second European Conference on Composite Materials (ECCM-II) : Volume 4.*" London, UK, (1987).

[5]   Hochard, Ch. and Thollon, Y. A generalized damage model for woven ply laminates under static and fatigue loading conditions. *International Journal of Fatigue* **32** (1), pp 158-165 (2010).

[6]   Varvani-Farahani, A. and Shirazi, A. A fatigue damage model for (0/90) FRP composites based on stiffness degradation of 0 degrees and 90 degrees composite plies. *Journal of Reinforced Plastics and Composites*, **26** (13) pp 1319-1336 (2007).

[7]   J.A.M. Ferreira, J.D.M. Costa , P.N.B. Reis , M.O.W. Richardson, Analysis of fatigue and damage in glass-®bre-reinforced polypropylene composite materials. *Composites Science and Technology,* **59** pp 1461-1467 (1999).

[8]   De Baere I., Van Paepegem W. Hochard C. and Degrieck J On the tension-tension fatigue behavior of a carbon reinforced thermoplastic part II: A dumbbell-shaped specimen. *Polymer Testing*, **30** (6), pp 663-672 (2011).

[9]   De Baere I., Van Paepegem W. Quaresimin M. and Degrieck J. On the tension-tension fatigue behavior of a carbon reinforced thermoplastic part I: limitations of the ASTM D3039/D3479 standard. *Polymer Testing*, **30** (6), pp 625-632 (2011).